

← → C Not secure | icovemat.uny.ac.id

ICoVEMAT INTERNATIONAL CONFERENCE ON VOCATIONAL EDUCATION OF MECHANICAL AND AUTOMOTIVE TECHNOLOGY

HOME CALL FOR PAPERS PAPER SUBMISSION COMMITTEE REGISTRATION FEE TIME & VENUE CONTACT US

CALL FOR PAPERS

5th INTERNATIONAL CONFERENCE on VOCATIONAL EDUCATION of MECHANICAL and AUTOMOTIVE TECHNOLOGY (ICoVEMAT) 2022

Full Paper Submission Deadline: Sept 25, 2022

Yogyakarta, Indonesia (Online) Oktober 6, 2022

Universitas Negeri Yogyakarta
Faculty of Engineering


Speakers:

- Prof. Jenq-Shiou Leu, Ph.D.
Department of Electronic and Computer Engineering,
National Taiwan University of Science and Technology, Taiwan
- Prof. Dr. Ing. Lee Seonha
Department of Construction and Environmental Engineering
Kongju National University, Republic of Korea
- Prof. Dr. Ing. Oliver Michler
Institut für Verkehrstelematik,
Technische Universität Dresden, Germany
- Associate Professor Ferry Jie, Ph.D, FCILT, FCES.
Edith Cowan University, Australia



home

5th INTERNATIONAL CONFERENCE on VOCATIONAL EDUCATION of MECHANICAL and AUTOMOTIVE TECHNOLOGY (ICoVEMAT) 2022




Yogyakarta, October 6, 2022
Universitas Negeri Yogyakarta


Theme :

Green Technology on Automotive and Manufacture for Sustainability Life


Speakers :




Taiwan




Department of Construction and Environmental Engineering,
Kongju National University, Republic of Korea



Prof. Dr. Ing. Oliver Michler
Institut für Verkehrstelematik, Technische
Universität Dresden, Germany



Associate Professor Ferry Jie, Ph.D, FCILT, FCES.
Edith Cowan University, Australia



Dr. Eng. Ir. Didik Nurhadiyanto, M.T., IPU
Department of Mechanical Engineering Education, Faculty of
Engineering, Universitas Negeri Yogyakarta, Indonesia

ONLINE REGISTRATION

User login

Username *

Password *

- Create new account
- Request new password

Security

Code *

5	9	6
7	1	2
3	4	8

List Of :

PRESENTERS

PARTICIPANTS

PREVIOUS EVENT:

Proceeding 3rd ICoVEMAT 2020
(Indexed by Scopus)

Proceeding 2nd ICoVEMAT 2019
(Indexed by Scopus)

Proceeding 1st ICoVEMAT 2018
(Indexed by Scopus)

Background

Research in manufacturing covers many aspects, including: additive manufacturing, automation and robotics, advanced materials, sensors and data analysis, augmented and virtual reality. Based on the results of research in this field, the manufacturing process of a product will be more effective and efficient. The automotive manufacturing industry is now able to make products faster because of this research. A car factory in Indonesia is supported by modern equipment and high technology in every stage of its process, with 40 percent of the total production process using robots. These processes include: Stamping, Welding, Painting, and Assembling. Innovation has many definitions. New products, process and business models that deliver commercial value and catalyse growth opportunities. Manufacturing innovation promise to impact every aspect of the manufacturing businesses, from design, research and development, production, supply chain and logistics management through to sales, marketing and even end of life management. These innovations will create highly intelligent, information-driven factories and distributed business models that can respond rapidly to change and deliver entirely new customised smart products and services (<https://www.imcrc.org/manufacturing-innovation/>).

Therefore, the Mechanical and Automotive Engineering Education Department, Universitas Negeri Yogyakarta organize the 5th International Conference on Vocational Education of Mechanical and Automotive Technology (ICOVEMAT) 2022. The aim of the 5th ICOVEMAT 2022 is to provide a platform for educators, academicians, researchers, and industry professionals from all over the world to share their idea, research results, and discuss the research and innovation in mechanical and automotive technology. It also provides an opportunity for participants to find global partners for future collaboration. We invite you to join us on 6th, October 2022 in Yogyakarta, Indonesia.

TIME SCHEDULE

Time (WIB)	Agenda
07.00 - 08.00	Registration
	all participants joint in zoom meeting https://uny.id/ictvt2022
	https://uny.id/ictvt2022 Meeting ID: 927 9625 4182 Passcode: ICTVT2022
08.00 - 08.05	Opening and Nation Anthem "Indonesia Raya"
08.05 - 08.10	Welcome Speech Chairman Organizer of by Dean of Faculty of Engineering
08.10 - 08.20	Welcome and Opening Speech by Rector of Universitas Negeri Yogyakarta
08.20 - 08.40	Keynote Speaker Prof. Dr. Muhadjir Effendy, M.A.P. (Coordinating Minister for Human Development and Culture of Indonesia)
08.40 - 09.20	Plenary Session I Moderator: Yuyun Yulia, M.Pd., Ph.D. (Vice Rector of Cooperation and Public Relation Affairs, Universitas Sarjanawiyata Tamansiswa, Indonesia) Speaker 1 : Prof. Jenq-Shiou Leu, Ph.D. (Department of Electronic and Computer Engineering, National Taiwan University of Science and Technology, Taiwan) Speaker 2 : Prof. Dr. Ing. Ir. Didik Nurhadyanto, M.T., IPU (Department of Mechanical Engineering Education, Universitas Negeri Yogyakarta, Indonesia)
09.20 - 10.00	Discussion
10.00 - 11.00	Plenary Session II Moderator : Dr. Phil. Ir. Didik Hariyanto, S.Pd.T., M.T. (Universitas Negeri Yogyakarta, Indonesia) Speaker 3 : Assoc. Prof. Ferry Jie, PhD, FCILT, FCES (Edith Cowan University, Australia) Speaker 4 : Prof. Dr. Ing. Lee Seonha (Department of Construction and Environmental Engineering, Kongju National University, Republic of Korea) Speaker 5 : Prof. Dr. Ing. Oliver Michler (Institut für Verkehrstelematik, Technische Universität Dresden, Germany)
11.00 - 12.00	Discussion
12.00 - 13.00	Lunch Break
13.00 - 16.30	Parallel Session https://bit.ly/icovemat2022 Meeting ID: 937 5372 3586 Passcode: icovemat

GROUP OF PARALLEL SESSION

ROOM A			
No	Author	Institution	Title of Paper
1	Muhammad Syawal Bin Mat Jahak	Universiti Malaysia Pahang	Evaluation of Transient Temperature Rise of MY1016 DC Motor in Standard Cycle
	Mohd Azri Hizami Bin Rasid	Universiti Malaysia Pahang	
	Sutiman	Universitas Negeri Yogyakarta	
2	Herminarto Sofyan	Universitas Negeri Yogyakarta	The Effect of Resin Ratio and Hardener Matrix Epoxy on the Carbon Fiber Composite Tensile Force
	Sukaswanto	Universitas Negeri Yogyakarta	
	Resa Agus Setyawan	Universitas Negeri Yogyakarta	
	Muhammad Nurdin Wahid	Universitas Negeri Yogyakarta	
3	I Wayan Warsita	Universitas Negeri Yogyakarta	Current Working Point Effect on BLDC Motor Temperature and Efficiency
	I Wayan Adiyasa	Universitas Negeri Yogyakarta	
	Mohd Azri Hizami Razid	Universiti Malaysia Pahang	
4	Ms. Ayu Sandra Dewi	Universitas Negeri Yogyakarta	BLDC Motor Performance Modeling for Electric Vehicles Based on Battery Performance
	Mr. I Wayan Adiyasa	Universitas Negeri Yogyakarta	
	Tafakur	Universitas Negeri Yogyakarta	
5	I Wayan Adiyasa	Universitas Negeri Yogyakarta	Analysis of Solar and Wind Energy Potential on the Design of a 16 kWh Swab Battery Charging System
	Yogi Arta	Politeknik Transportasi Darat Bali	
	Rai Pramesti	Universitas Brawijaya	

6	Syaian Nur Fajri	National Yunlin University of Science and Technology	Development of Pole-Piece Shapes in Coaxial Magnetic Gears
	Ibnu Siswanto	Universitas Negeri Yogyakarta	
7	Agung Prasetyo	Universitas Negeri Yogyakarta	Electrical System of Prototype Electric Vehicle for Disable
	Ibnu Siswanto	Universitas Negeri Yogyakarta	
	Abdulah Syafiq	National Central University	
	Fajar Ardian Ikhwanasyah	Universitas Negeri Yogyakarta	

ROOM B

1	Sutiman	Universitas Negeri Yogyakarta	The Effect of Increasing the Compression Ratio on Performance and Fuel Consumption on Yamaha Vega Force FI Engines with Ethanol Fuel
	Gargazi	Universitas Mandalika Mataram	
	Nur Arifin	Universitas Negeri Yogyakarta	
	Julian Fathi	Universitas Negeri Yogyakarta	
2	Zainal Arifin	Universitas Negeri Yogyakarta	The Effect of Gear Ratio Changes on Acceleration Performance in EV 22 Garuda UNY Team Car Based on Matlab Simulink Modeling Results
	Yosep Efendi	Universitas Negeri Yogyakarta	
	Agus Budiman	Universitas Negeri Yogyakarta	
3	Muhkamad Wakid	Universitas Negeri Yogyakarta	The Effect of Toe Adjustment on the Garuda Urban Gasoline 2020 (UG 20) Vehicle Glide Distance
	Zainal Arifin	Universitas Negeri Yogyakarta	
	Anton Dwi Mantoro	Universitas Negeri Yogyakarta	
	Yoga Guntur Sampurno	Universitas Negeri Yogyakarta	
4	Ardiyan Rifki Stevanni	Universitas Negeri Yogyakarta	The Effect of Variations Ignition Timing on Characteristics And Exhaust Emission on Yamaha Vega Force FI Engines Using

5	Beny Dwipa	Politeknik Transportasi Darat Bali	Ethanol Fuel (E100)
	Sudarwanto	Universitas Negeri Yogyakarta	Injection Duration Mapping Effect on K0J Engine Power and Fuel Consumption
	Beny Setya Nugraha	Universitas Negeri Yogyakarta	
	Agung Prayoga	Universitas Negeri Yogyakarta	
	Muhammad Partono	Universitas Negeri Yogyakarta	The Effect of Tire Pressure on Car Fuel Consumption Garuda Urban Gasoline 19, in The Shell Eco-Marathon Competition Asia 2019, Malaysia
Kir Haryana	Universitas Negeri Yogyakarta		
Zainal Arifin	Universitas Negeri Yogyakarta		
Ilham Nofi Yoga	Universitas Negeri Yogyakarta		
7	Nafis Wahyu Purnomo	Universitas Negeri Yogyakarta	Mapping The Injection Duration of Yamaha Vega Force FI Engine With Ethanol Fuel
	Muhammad Zidan Naresworo	Universitas Negeri Yogyakarta	
	Tafakur	Universitas Negeri Yogyakarta	
7	Teguh Setiyawan Nurhidayah	Universitas Negeri Yogyakarta	Mapping The Injection Duration of Yamaha Vega Force FI Engine With Ethanol Fuel
	I Kadek Bagus Suryanata	Universitas Negeri Yogyakarta	

ROOM C

1	Teguh Arifin	Akademi Komunitas Negeri Pacitan	FRONT AERODYNAMIC SYSTEM DEVELOPMENT OF FORMULA GARUDA 18 (FG18) CAR USING COMPUTATIONAL FLUID DYNAMIC FOR FORMULA SAE
	Zainal Arifin	Universitas Negeri Yogyakarta	
	Sutiman	Universitas Negeri Yogyakarta	
	Yoga Arob Wicaksono	Akademi Komunitas Negeri Pacitan	
	Suhartanta	Universitas Negeri Yogyakarta	
	Amir Fatah	Universitas Negeri Yogyakarta	

2	Amir Fatah	Universitas Negeri Yogyakarta	Vehicle Driving Techniques for the Urban Gasoline Category of the 2019 Shell Eco-marathon Asia
	Rizki Septiana	Universitas Negeri Yogyakarta	
	Dhimas Derra Adipratama	Universitas Negeri Yogyakarta	
3	Moch Solikin	Universitas Negeri Yogyakarta	Intake Plenum Design Effect on Husqvarna SM630 Engine Power, Applied in The Formula Garuda UNY Vehicle
	Irfan Muhammad Farid	Universitas Negeri Yogyakarta	
	I Wayan Warsita	Universitas Negeri Yogyakarta	
4	Gunadi	Universitas Negeri Yogyakarta	The Effect of Swing Arm Design on Double Wishbone Suspension on Changes in Roll Center and Camber Gain of Formula Student Cars
	Martubi	Universitas Negeri Yogyakarta	
	Muhammad Ragil Tri Atmaja	Universitas Negeri Yogyakarta	
	Christopher Yonathan Ie	Universitas Negeri Yogyakarta	
5	Ibnu Siswanto	Universitas Negeri Yogyakarta	Analysis of the Effect of Materials on Heat Distribution in the Design of Battery Pack Cases for the Garuda Kencana Electric Car 2022
	I Wayan Adiyasa	Universitas Negeri Yogyakarta	
	Satria Elang Nugraha	Universitas Negeri Yogyakarta	
6	Naufal Annas Fauzi	Universitas Negeri Yogyakarta	Impact of implementing large-scale Social Restrictions due to COVID-19 on Ambient Air Quality in Yogyakarta Parameters SO ₂ , NO ₂ , and CO
	Joko Sriyanto	Universitas Negeri Yogyakarta	
	Yosep Efendi	Universitas Negeri Yogyakarta	
	Sutiman	Universitas Negeri Yogyakarta	

7	Khusni Syaqui	Universitas Negeri Yogyakarta	Pulley Design as Powertrain Mechanism in a Wheelchair Portable Electric Motor
	Surono	Universitas Negeri Yogyakarta	
	Angga Damayanto	Universitas Negeri Yogyakarta	
	Rizky Avika	Universitas Negeri Yogyakarta	
	Amry Muhammad Azhzhahar	Universitas Negeri Yogyakarta	
	Ari Fajar Ananto	Universitas Negeri Yogyakarta	
ROOM D			
1	SUNARYO	Universitas Sains AL-Qur'an	CHARACTERIZATION OF INDONESIAN NATURAL ZEOLITE AS CATALYST FOR WASTE PYROLYSIS PROCESS
	Hermawan	Universitas Sains AL-Qur'an	
	Akhmad Irfan	Universitas Sains AL-Qur'an	
	Suyitno	Universitas Sebelas Maret	
2	Agus Widianto	Universitas Negeri Yogyakarta	Prediction of Weld Quality of Micro Friction Stir Spot Welding (µFSSW) on Similar Materials AZ31B Using Fuzzy Logic
	Herminarto Sofyan,	Universitas Negeri Yogyakarta	
	Gunadi	Universitas Negeri Yogyakarta	
	Aan Yudianto	Universitas Negeri Yogyakarta	
3	Semuel Boron Membala	Hasanuddin University	Graphite Coating of Aluminum Bipolar Plate Using Compression Molding Method
	Rieza Zulrian Aldio	Universitas Islam Riau	
	Dedikarni	Universitas Islam Riau	
	Deni Restu Fauzi	Universitas Islam Riau	
	Sutiman	Universitas Negeri Yogyakarta	

4	Yoga Guntur Sampurno	Universitas Negeri Yogyakarta	The Effect of Epoxy Resin And Hardener Matrix Ratio With Vacuum Assisted Resin Transfer Molding Method on Mechanical Properties of Carbon Fiber Composite
	Donny Fernandez	Universitas Negeri Yogyakarta	
	Ahmad Yoga Pradana	Universitas Negeri Yogyakarta	
	Kesit Bayu Purnomo	Universitas Negeri Yogyakarta	
5	Zainal Arifin	Universitas Negeri Yogyakarta	Cost Report Analysis On The Material and Steering Manufacturing Process Of Formula Garuda 2019 (FG-19) Vehicle Garuda UNY Racing Team
	I Kadek Warjaya	Universitas Negeri Yogyakarta	
	Nur Khamdan	Universitas Negeri Yogyakarta	
	Rizky Avika	Universitas Negeri Yogyakarta	
6	Gunadi	Universitas Negeri Yogyakarta	The Effect Carbon Fiber Composite with Core Variations on Flexural Strength and Density on The Reinforcement of The Urban Vehicle Garuda UNY
	Faiz Aryasatya Muzakki	Universitas Negeri Yogyakarta	
	I Kadek Warjaya	Universitas Negeri Yogyakarta	
7	Adhy Wahyu Nugroho	Universitas Negeri Yogyakarta	Performance Analysis of Throttle by Wire using DC and BLDC Motor Actuator
	I Kadek Warjaya	Universitas Negeri Yogyakarta	
	I Wayan Adiyasa	Universitas Negeri Yogyakarta	
	Khalid Himawan	Universitas Negeri Yogyakarta	

Effect of various repetition coating and thickness of YSB electrolyte on the electrochemical performance of the single button cell solid oxide fuel cell

Dedikarni Panuh ^{a,c*}, Dody Yulianto ^a, M. F. Shukur ^b, Andanastuti Muchtar ^a,

^aDepartment of Mechanical Engineering, Faculty of Engineering, Universitas Islam Riau, Indonesia

^bFundamental and Applied Sciences Department Universiti Teknologi Petronas, Seri Iskandar, Malaysia

^cFuel Cell Institute, Universiti Kebangsaan Malaysia, 43600 UKM Bangi, Selangor, Malaysia

*Corresponding Author: dedikarni@eng.uir.ac.id

ABSTRACT

Reducing the operating temperature and optimization design while maintaining high cell performance is the primary consideration in designing current SOFCs. The effect of the electrolyte YSB thickness on the electrochemical performance of the single cell was measured from 500–650°C was studied in detail. Cell performance testing was performed using impedance for electrochemical characterization and single-cell capability testing. The YSB electrolyte coated on the NiO–SDC | SDC substrates was deposited as a thin film with varying thicknesses of 1.5, 3.5, 5.5, and 7.5 µm after 1, 2, 3, and 4 applications of coatings, respectively, at a sintering temperature of 800°C for two h. These findings confirmed that the number of layers was proportional to the thickness of the YSB electrolyte. The results indicated that the bilayer electrolyte system of $Y_{0.25}Bi_{0.75}O_{1.5}/Sm_{0.2}Ce_{0.8}O_{1.90}$ with three applications of coating at 650°C exhibited optimum current and power densities of 228 mA/cm² and 82 mW/cm², respectively. The interfacial polarization cells achieved a low total resistance (0.55 Ωcm²) and a high open circuit potential (1.092 V) after three coating applications with 5–6 µm thickness at 600°C. This study produced a single button cell system with a total deficient cell interfacial resistance compared to the previous studies on intermediate and low-temperature SOFCs.

Key Words: SOFC, Bilayer Electrolyte, SDC, YSB.

Introduction

High operating temperature is one of the main barriers to the wide-scale adoption of solid oxide fuel cell (SOFC) technology [1]. Therefore, most research focused on developing low-intermediate temperature SOFC operating at around range temperature 500-600 [2]. To achieve low-intermediate temperatures, several from the viewpoint of new materials, novel processes, and unique architectures must be re-examined [3].

Recently most research and development activities on SOFC are mainly focused on the commercially viable SOFC manufacturing technology with high electrochemical performance, the transformation of stack design, and cost-effective process. In fabrications, p has been proposed and developed for SOFC. Various are available for depositing films on dense or porous substrates based on ceramic powder techniques or chemical and physical processes. These methods include electrochemical vapor deposition, chemical vapor deposition, physical vapor deposition (radio frequency and magnetron sputtering), laser ablation, plasma spraying, and depositing techniques [4][5].

Although the methods mentioned above are well established, the investment cost for the apparatus is higher than those used in the dip coating method. Dip coating is expected to produce a satisfactory surface condition in the fabrication of YSB bilayered composite film electrolyte on the SDC electrolyte because the thickness of the electrolyte substrate can be easily controlled through the number of dip coatings. This technique is the simplest and the most appropriate method for preparing films with large surface areas [6]. Furthermore, dip coating is inexpensive and more suitable for mass production, even in multi-layer cells.

Electrolyte thickness is essential and must be considered because surface morphology has a vital function in the physical and chemical properties of the bilayer electrolyte [7][8]. However, details of the optimum thickness and electrochemical properties of YSB composite electrolytes on SDC/YSB bilayered electrolytes are scarce. This study aims to determine the influence of SDC/YSB bilayered combined electrolyte thickness on the interfacial polarization resistance and electrochemical performance of single SOFC cells with SDC/YSB as a bilayered electrolyte, Ag-YSB composite as cathode and NiO–SDC as an anode.

Experiment Procedure

2.1 Materials and specimen preparation

Commercial material available yttrium oxide (99.999 wt%) and bismuth (III) oxide (99.999 wt%, Sigma Aldrich Sdn. Bhd) was mixed at a molar ratio 1 of : 3. The powder and Zirconia ball (Fritsch Pulverisette 6) in ethanol was combined with mechanical mill method for 24 h, and then calcined in air at 750 °C. This-gel practice prepares three-element SDC powder with (Ce_{0.8}sol-gel_{1.9}) d [9].

NiO, Nickel (II) Oxide (99.8 wt%, Sigma Aldrich Sdn. Bhd), and SDC powder were mixed at a weight ratio of 60:40 and were prepared by ball milling in ethanol for 24 h. NiO-SDC powers were mixed with zirconia ball medium, dried in an oven at 80 °C for 12 h, and thoroughly ground. The dried powders were then heated and called at 1100°C for 5 hours to obtain NiO-SDC composite powder.

To prepare the Ag-YSB cathode slurry, silver (I) oxide (99.8 wt%, Sigma Aldrich Sdn. Bhd) and YSB were added at a weight ratio of 50:50. The α -terpineol, di-n-butyl phthalate (Merck Sdn. Bhd), and polyvinyl butyral (PVB) (Sigma) as organics binder were mixed at a volume ratio 3: 1: 2. The organics binder was ma mixture with agate mortar in ethanol as a dispersing medium for 30 min.

2.2 Characterization

The microstructure of single button cells SOFC samples was observed using field emission scanning electron microscopy (FESEM), and the formation of different phases by the Ag-YSB, YSB, SDC, and NiO/SDC system during the coating of bilayer electrolyte films was investigated using X-ray diffraction (XRD) and electrochemical impedance spectroscopy (EIS). The temperature and mass loss with phase transformation was determined by gravimetric analysis and differential scanning calorimetry (TGA and DSC Jupiter 449F3) from 30 °C to 1200 °C. The phase of the cathode was analyzed using XRD (semen D-500) with Cu K α at a 2 θ range from an angle of 20° to 80°, and the Rietveld method using the EVA software were obtained pattern refinements. The morphology and grain size of the composite cathode pellets was observed using a Scanning electron microscope (Zeiss EVA MA10) with 15 XK magnification.

2.3 Button single-cell fabrication, performance, and electrochemical measurement

The NiO-SDC anode and the SDC electrolyte pellets were co-pressing by cold pressing. The pellet was used as a substrate or half-cell (25 mm diameter and sintered at 1400°C for five h). The NiO-SDC anode and SDC/YSB bilayered electrolyte (half Cell) were coated with Ag-YSB cathode slurry using SPM. The Ag_2O_3 and YSB powder as composite cathode and organic binder were mixed by SPM, then deposited onto the substrate surface. The slurry containing the composite and organic binder desired to make the solid deposited film by a chemical reaction method. And then, the influence of the coating process on thickness layers was investigated with four times repetitions. By sintering, the composite cathode fabricates at 800 °C for two h in air. The complete single SOFC button cell system became the end product system. The final configuration button single cell (NiO-SDC/SDC/YSB/Ag-YSB) based on substrate SDC/YSB as a bilayer electrolyte is shown in fig 1.

The half cell with Ag-YSB composite cathode was measured electrochemical performance (interfacial polarization resistance, R_p) using EIS Autolab Nova 1.8 Model PGSTAT302N). The impression of repetition of coating and temperature on cell performance was assessed using impedance spectroscopy. This test has been widely used to determine the achievements of solid oxide fuel cells involving more complex curvature (arc) with various processes and materials used in making single cells. Different cell manufacturing processes have contributed to a more complex impedance spectrum. The impedance spectrum has been used to separate and identify the bulk interfacial polarization resistance (R_p Total, Report), the constant phase element (CPE), and the interfacial polarization resistance (R_p) in the range of 0.01 Hz to 10 kHz.

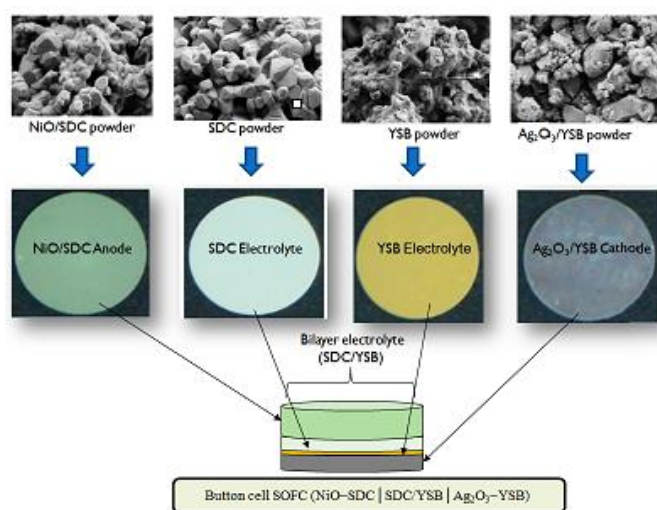


Fig. 1 A schematic configuration of NiO-SDC/SDC/YSB/Ag-YSB as a button

single cell SOFC.

4. Result and discussion

4.1 Button Single-Cell Performance Analysis

The performance of cells is shown in Figure 2, with hydrogen and pure oxygen as oxides. Performance measurements were performed at operating temperatures of 600°C.

Studies on the effect of YSB electrolyte thickness on the surface of the SDC electrolyte in the form of NiO–SDC | SDC/YSB | Ag₂O₃–YSB single cell. NiO–SDC anode is a supporting substrate, and Ag₂O₃–YSB is a cathode. The current density and voltage (I-V) performance on YSB thickness was conducted with NiO–SDC | SDC/YSB | Ag₂O₃–YSB single-cell anode support. YSB electrolyte performance testing can be performed when a cell is designed with SDC electrolyte on the anode surface, and YSB is coated on the cathode surface to stabilize YSB and SDC under oxygen reduction (P_{O_2}) conditions [10][11].

The results of the performance tests of open-circuit potential (OCP), current density (I), and power density (P) of cells at 600°C are shown in Figure 2 (a). The maximum power density of a single cell NiO–SDC | SDC/YSB | Ag₂O₃–YSB with a single YSB electrolyte coating was 66.1 mW/cm², and the maximum current density was 188 mA/cm² at 600°C.

The result of the measurement of the maximum power density in the second YSB electrolyte coating with a yield of 72 mW/cm² and the maximum current thickness was 212.2 mA/cm² as shown in Figure 2 (b). Figure 2 (c) shows the results of the measurement of maximum power density during the third YSB electrolyte coating of 82 mW/cm² and maximum current thickness with yields of 225.3 mA/cm². Figure 2 (d) shows the results of measuring the maximum power density at four times the YSB electrolyte coating is 80 mW/cm² and the maximum current density is 218.7 mA/cm². Increased OCP (Volt), I (mA/cm²), and P (mW/cm²) values from one coating to the fourth coating, as shown in Figure 2. The maximum power density was obtained at an operating temperature of 600°C with an average electrolyte thickness (YSB) of 5.5 μm, which was the third time. Subsequently, OCP, I-V, power density, and ty values began declining during the fourth coating. In parallel with the FESEM thickness test, four coating times produced YSB electrolyte thickness at an average thickness of 7.5 μm. The effect of increasing the number of coatings on the OCP value, current density, and single-cell power developed is shown in Figure 2. The maximum voltage value, power density, and present are obtained by optimizing the YSB electrolyte thickness value. The increase in V

(Volt), I (mA/cm^2), and P (mW/cm^2) values of the YSB electrolyte thickness change is evidence that YSB electrolytes have successfully inhibited electrolyte conductivity (SDC) since the reduction of Ce^{4+} to Ce^{3+} did not occur in the interface area so that it does not affect cell performance. Increased voltage, current, and power values are also observed in ESB/GDC double-layer thin film electrolytes [12]. Ahn et al. (2009) [12] reported that ESB thin film electrolytes were produced on the surface of GDC electrolytes using a physical vapor deposition (PVD) method. Ahn et al. (2009) also reported that the performance of single button cells with double-layer electrolyte thin film (ESB/GDC) film ($\sim 10 / \sim 4 \mu\text{m}$) resulted in an OCP increase of 0.72 to 0.77 V.

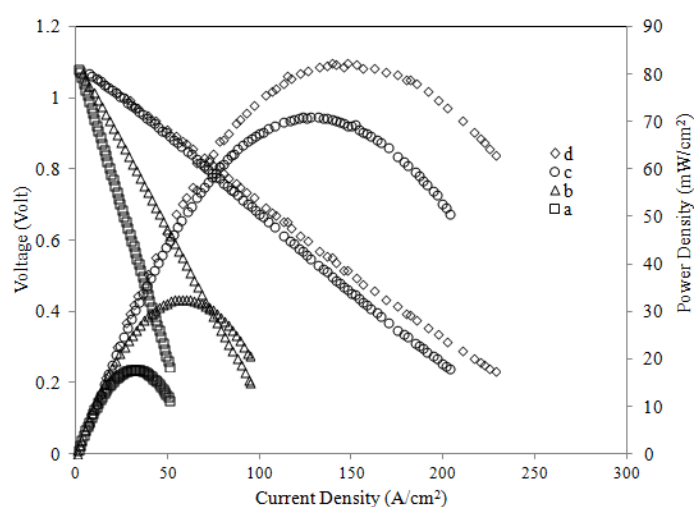


Figure 2 Current (I) –Voltage (V) performance test with (a) one, (b) two, (c) three, (d) four YSB coating times the bilayer electrolyte

The average OCP for various repeats of YSB electrolyte coating on the surface of the SDC electrolyte is shown in Figure 3. OCP values in one coating up to four times coating are 1.068 V, 1.072 V, 1.092 V, and 1.084 V. OCP, I-V values, and optimum power density are in the third coating with moderate operating temperature ($600 \text{ }^\circ\text{C}$) with OCP value of 1.092 V, a current density of $0.23 \text{ mA}/\text{cm}^2$ and a power density of $82 \text{ mW}/\text{cm}^2$. Increasing the number of coatings up to three repetitions increased the OCP value to 1.092 V. The optimum coating thickness was performed three times to repeat the YSB electrolyte coating on the surface of the SDC electrolyte and produced a YSB electrolyte thickness of $5.5 \mu\text{m}$. Increased OCP value, up to 1.092 V, current density $0.23 \text{ mA}/\text{cm}^2$ and power density $82 \text{ mW}/\text{cm}^2$. The SDC, in this case, produced an oxygen vacancy in which three O^{2-} ions replaced four O^2 ions. The emptiness

of the oxygen site has led to the movement of electrons and the increase in ion flow in the electrolyte. SDC is a highly ionic conductivity material with a readily available oxygen atom in which the movement causes ion flow.

Optimum coating and thickness have resulted in maximum OCP value. However, the fourth coating decreased the OCP value to 1.084 V. Increasing the thickness to 7.5 μm in the fourth coating decreased the OCP value. This condition occurs when the YSB electrolyte thickness exceeds the optimum thickness, and the YSB electrolyte begins to decompose. In SDC electrolytes, Ce^{4+} to Ce^{3+} electrons were decreased at low oxygen partial pressure and mixing of ion and electron conductance. Mixing electrons and ions with high-performance electrolytes has led to short circuits and decreased cell performance. YSB electrolyte thin films can prevent the cell from degrading and inhibiting electrolyte conductance across the electrolyte. YSB electrolytes are used to suppress electron conductivity from the substrate, and YSB thin layers are also used to produce high ion conductance. The SDC layer acts as a support for the YSB to be stable and stable [13].

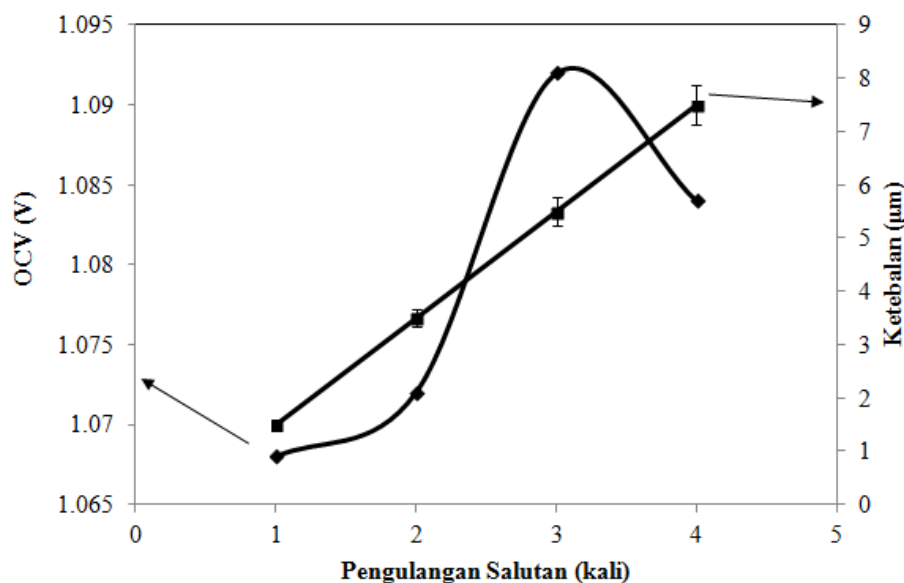


Figure 3 Average OCP for various repetition coating and thickness of YSB electrolyte on SDC electrolyte surface

Bilayer electrolyte analysis for YSB / SDC has also been investigated by Virkar (1991) [14], Huang et al. (2008) [15], and Zhang et al. (2011) [13]. Oxygen partial pressure (P_{O_2}) values of two electrolytes were determined by the electrolyte thickness ratio and ion and electron conductivity of both electrolytes. The use of thin layers of SDC $<10 \mu\text{m}$ and YSB $<6 \mu\text{m}$ gave a low resistance drop and provided control to the surface for no degradation. This is because the oxygen partial pressure (P_{O_2}) interfacial with the SDC is further. The thickness of

YSB $<6 \mu\text{m}$ and SDC $<10 \mu\text{m}$ protected the electrolyte in bulk. However, if a very thick YSB film is found, it can increase the electrolyte resistance and cause a decrease in ion conductivity. YSB electrolyte films that are too thick also make YSB easy to decompose. This is due to the oxygen partial pressure (P_{O_2}) and the rising temperature of the environment.

4.2 Impedance spectroscopy analysis

Four impedance spectra with one repetition of the coating to four times the layer, as shown in Figure 4. Each repetition of the coating consists of three overlapping arcs. Figure 4 (a) shows the impedance spectrum with one coating. Three turns in the figure with a larger diameter than the YSB electrolyte as a second coating. This condition indicates a more significant overall coating than the second YSB electrolyte coating. Figure 4 (b) shows the impedance spectrum with twice the layer. The figure showed three arcs with smaller diameters than the YSB electrolyte coating for the first repetition and more significant than the third coating.

This phenomenon shows that the overall resistance in the second coating is smaller than the one coating, and the thick one is the YSB electrolyte coating a third time. Figure 4 (c) shows the impedance spectrum with three times the layer. The figure showed three half rounds with smaller diameters than all YSB electrolyte coatings. This condition applies because three times, the coating is sufficient to cover the entire surface of the SDC electrolyte with the optimum coating thickness and gives the lowest overall resistance; Rajah 4 (d) shows the impedance spectrum with four times the YSB electrolyte coating on the SDC surface. Impedance spectrum at one time coating so that four times the coating exhibited a decrease in half size and increased initially at the fourth time coating. This phenomenon holds because the increase in layer gives the impression of decreasing the overall barrier of cells so that optimum thickness is achieved. This condition is indicated by the decrease in size halfway around between the third coating is more closely matched so that it overlaps on the bulk resistance (R_b) and the electrode resistance (R_e), and the repetition of the layer has reached the optimum thickness three times to produce a decrease in minimum resistance. However, the overall resistance has reincreased for the fourth time. This condition is shown by the enlargement of half the size of the electrode resistance (R_e).

The first arc for a real axis at high frequencies is the ohm resistance (R_s) contributed by the wire and cell resistance. In this study, the platinum mode is connected to the outer circuit to determine the value of resistance, OCP, power, and current density. Interfacial polarization resistance (R_p), R_p is the bulk resistance (R_{bulk} , R_b) + grain boundary resistance (R_{grain}),

R_g) + resistance electrode ($R_{\text{elektrode}}$, R_e), and the total polarization resistance (R_{polar}) is $R_s + R_p$. All these resistance are known to use Autolab with Nova 1.5 software in the form of equal spectra and circuits to obtain the value of each coated resistance.

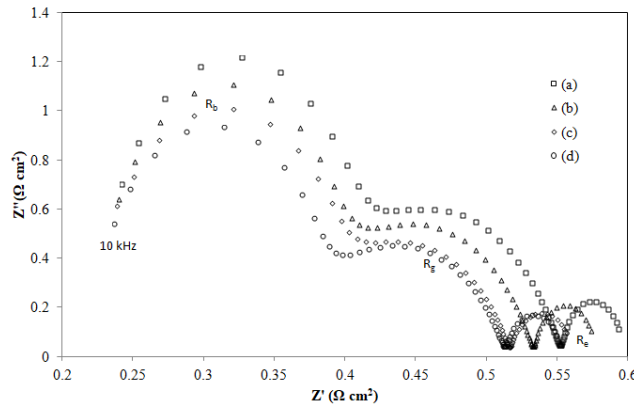


Figure 4 The impedance spectrum shows the variety of coating repetitions: (a) once, (b) twice, (c) three times, and (d) four times.

The impedance spectral equivalent circuit of SOFC single button cells with YSB electrolyte thickness at one time repeated coating up to four times with coating resistance total (R_{polar}), $0.6 \Omega\text{cm}^2$, $0.56 \Omega\text{cm}^2$, $0.55 \Omega\text{cm}^2$ and $0.58 \Omega\text{cm}^2$ and interfacial resistance (R_p) $0.37 \Omega\text{cm}^2$, $0.34 \Omega\text{cm}^2$, $0.33 \Omega\text{cm}^2$, $0.35 \Omega\text{cm}^2$ as shown in Figure 5 and 6. However, different electrolyte layer thicknesses do not have a significant impact on the ohm resistance (R_s) values of $0.228 \Omega\text{cm}^2$, $0.225 \Omega\text{cm}^2$, $0.224 \Omega\text{cm}^2$ and $0.227 \Omega\text{cm}^2$ as the ohm resistance value is related to the interconnect wire between the cell and the outer circuit. In this study, the value of the ohm resistance has little effect on the overall resistance and can be ignored because the same connection wire is used every time a test is used. Therefore, modification of the ohm resistance is unnecessary as it does not significantly impact the system as a whole.

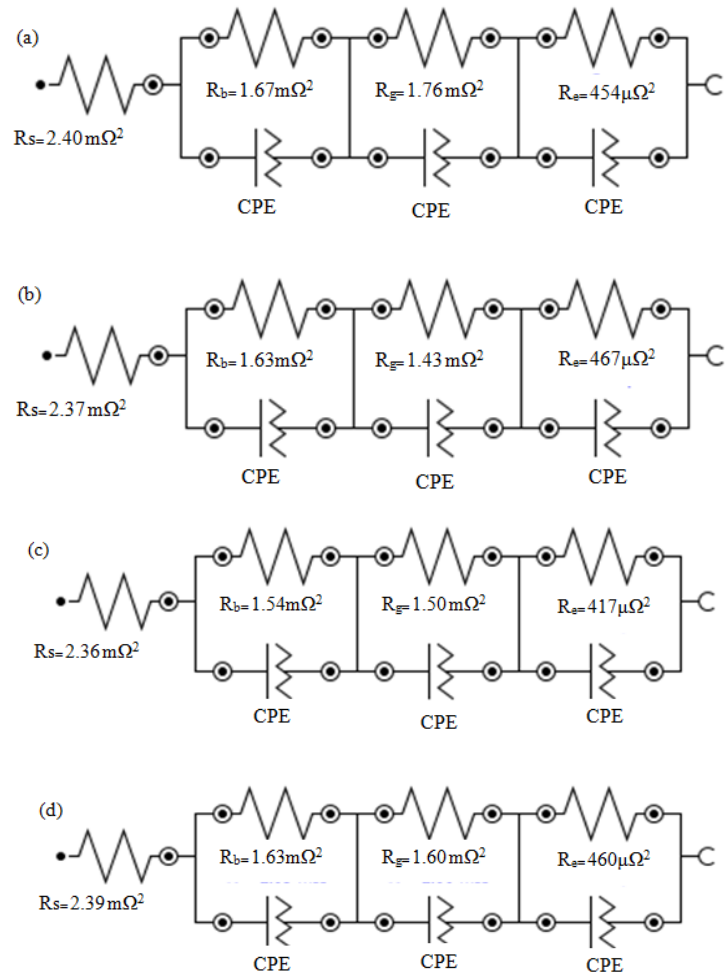


Figure 5 Impedance spectrum equivalent circuits based on various coating repetitions: (a) once, (b) twice, (c) three times, and (d) four times.

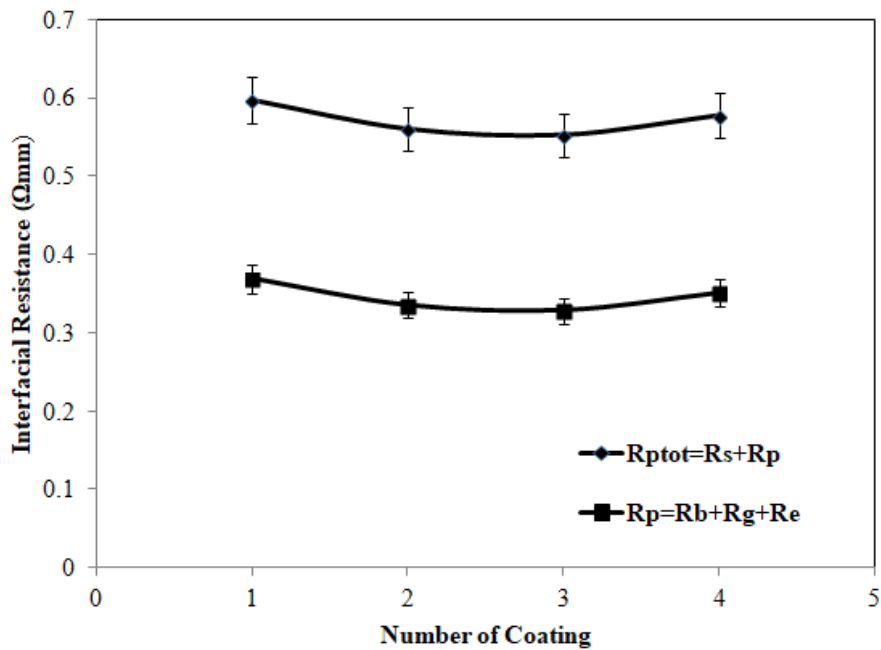


Figure 6 Total interfacial polarization resistance ($R_{p_{tot}}$) and bulk interface polarization resistance (R_p) at various coating repetitions: (a) once, (b) twice, (c) three times, and (d) four times.

The addition of the YSB electrolyte coating up to 4 times reduced the interfacial resistance value (R_p) contributed by the grain resistance (Rebound, R_g) and the electrode resistance (Relectrode, R_e). YSB electrolyte coating produced a $0.60 \Omega\text{cm}^2$ polishing interfacial and dropped to $0.55 \Omega\text{cm}^2$ on the third coating. The third coating with a thickness of $5.5 \mu\text{m}$ gave the lowest R_p value, and the interface resistance increased again to $0.58 \Omega\text{cm}^2$ on the fourth coating. The addition of YSB electrolyte coating on the surface of the SDC electrolyte affected the interfacial polarization resistance (R_p). The three-coating addition of YSB electrolyte coating reduced the opposition to a minimum because the third coating successfully thinned the entire surface of the SDC electrolyte and prevented the flow of electrons from the SDC electrolyte ideally. Two-layer electrolyte analysis for YSB/SDC was also studied by Virkar (1991)[14], Huang et al. (2008)[15], and Zhang et al. (2011) [13].

The oxygen partial pressure (P_{O_2}) of two electrolytes is determined by the ratio of electrolyte thickness and ion and electron conductivity of both electrolytes. The thickness of YSB $< 2 \mu\text{m}$ protected the electrolyte in bulk, and the CeO_3/YSB thickness ratio was large. If the oxygen partial pressure (P_{O_2}) interface is too close to the surface and the YSB film is insufficient to cover the ceria surface, then there is a decrease in the shear due to exposure to P_{O_2} . The use of a thin layer of fiber ($< 10 \mu\text{m}$) with a YSB thin layer of $< 6 \mu\text{m}$ gave a decreasing resistance and showed the control of the ceria no reduction, as the oxygen partial pressure (P_{O_2}) interfacial was closer to the fuel. However, adding up to four times the coating exceeds the maximum threshold, resulting in an increase in the polarization resistance of the interfacial. Excessive growth in the number of layers can also prevent the flow of electrons and ion conductance from the electrolyte to the cathode.

This decrease in the interfacial polarization resistance is due to the maximum ability of the YSB electrolyte to inhibit the conductivity of the SDC electrons across the YSB electrolyte. It is expected to increase the conductivity of the oxygen ions across the YSB electrolyte. The decreased R_p was also due to the compatibility between the YSB electrolyte and the Ag_2O_3 -YSB cathode. Using the same electrolyte and electrode materials is expected to facilitate the conductivity of oxygen ions from electrolytes with YSB material and cathode composites with YSB and Ag_2O_3 mixtures. According to the report of Zhang et al. (2010)[16] and Kenjo and

Kanehira (2002)[17], this phenomenon also occurs in LSM–YSB materials and YSB electrolytes. The decrease in R_p is due to the increase in oxygen ion conductance and chemical compatibility between the cathode material (LSM–YSB) and the YSB electrolyte. Chemical compatibility between cathode and electrolyte occurs when electrolytes and cathodes are based on the same material until the manufacture and operation of a single button cell do not occur, cracking and separation of each component due to different thermal expansion. Low and high-frequency intervals for interfacial polarization resistance (R_p) are also contributed by the anode and cathode [18]. In this study, the high frequency (1 kHz) and low (0.1 Hz) shortcuts occur on the Z' axis approaching $0.4 \Omega\text{cm}^2$.

The results of this study are compared to several previous studies with SDC/YSB bilayer-layer electrolytes at 0.5 mm SDC thickness and 5.5 μm YSB and Ag_2O_3 /YSB cathode material with an operating temperature of 600 °C as shown in Table 4.2. This study using YSB electrolyte materials yielded higher OCP results than previous research. Previous research reports by Wachsman et al. (1992) [19] on GDC/ESB bilayer-layer electrolytes at 0.9 μm GDC thickness and 50-60 μm ESB thickness with Au cathode materials gave an OCP value of up to 0.901-0.977 V. This is due to the unstable ceria and the use of Au as a cathode material as a good electron conductor

Park and Wachsman (2006)[20] investigated the SDC/ESB bilayer layer electrolyte at 1.5 μm SDC thickness and nine μm ESB with Au cathode material, giving OCP value up to 0.783 V. And then, Park and Wachsman (2006) investigated the SDC/ESB bilayer layer electrolyte at thickness 1.5 μm SDC and 22 μm ESB with Ag/YSB cathode material gave an OCP value of up to 0.949 V. The increase in ESB electrolyte thickness on the SDC surface resulted in an increase in OCP value from 0.783-0.949 V. The OCP value increase occurred due to the ESB increasing ion conductivity and did not occur because the SDC backing electrolyte successfully prevented YSB from decomposition.

Leng and Chan (2006) [21] investigated the bilayer-layer GDC/YSB electrolyte at GDC thickness of 84 μm and YSB 6 μm with Pt cathode material giving an OCP value of up to 0.885 V. Zhang et al. (2010) [16] investigated the bilayer-layer SDC/YSB electrolyte at SDC 26 and 6 μm thickness with LSM / YSB cathode material giving OCP values up to 0.897 V and Zhang et al. (2011)[13] investigated the bilayer-electrolyte at GDC/YSB thickness with GDC thickness of 26 μm and YSB 6 μm with Ag/YSB cathode material giving OCP value of up to

0.887 V. OCP value increase occurred in the event of a decrease in the support electrolyte thickness. This is due to the reduction of the supporting electrolyte thickness, which increases the conductivity of the ion from the cathode to the electrolyte. However, the use of not match electrolyte cathode material reduced the OCP value from 0.897-0.887 V. This is due to electrolyte material that does not fit the cathode and causes both components to not optimally, thus reducing cell performance. Therefore, it can be concluded that the performance value differences from some previous studies were due to different material selection parameters, manufacturing methods, and coating thickness. Optimization of material selection parameters, manufacturing methods, and coating thickness also contributed to the increased OCP value.

4 CONCLUSIONS

The $Y_{0.25}Bi_{0.75}O_{1.5}$ electrolyte (YSB) was used to suppress the electron conductivity of the substrate, and the YSB thin layer (5.5 μm) was used to produce high conductivity in the electrolyte. The YSB thin film electrolyte coating on the surface of the SDC electrolyte prevented Ce_2O_3 from being exposed to partial oxygen pressure. Increased OCP value, up to 1.092 V, current density 0.23 mA/cm^2 and power density 82 mW/cm^2 . The SDC, in this case, produced an oxygen vacancy in which three O^{2-} replaced four O^2 ions. The emptiness of the oxygen site has led to the movement of electrons and the increase in ion flow in the electrolyte. The YSB with the $Y_{0.25}Bi_{0.75}O_{1.5}$ system prevented the ceria (Ce_2O_3) from degrading (Ce^{4+} to Ce^{3+}) and restricted the electrons' conductivity across the electrolyte. The thick (0.5 mm) SDC layer acts as a YSB support for more OCP and stability single button solid oxide fuel cell.

ACKNOWLEDGMENTS

The author acknowledges Universiti Petronas Malaysia, the Universitas Islam Riau, for the matching grand research sponsorship under Nomor: 468/Kontrak/LPM-UIR-9-2018 and 361/Kontrak/LPPM-UIR/4-2018.

REFERENCES

- [1] S. P. S. Badwal and K. Foger, "Solid Oxide Electrolyte," *Ceram. Int.*, vol. 8842, no. 95, pp. 257–265, 1996.
- [2] K. Eguchi, T. Setoguchi, T. Inoue, and H. Arai, "Electrical properties of ceria-based oxides and their application to solid oxide fuel cells," *Solid State Ionics*, 1992.
- [3] D. Yang *et al.*, "Low-temperature solid oxide fuel cells with pulsed laser deposited bi-

- layer electrolyte,” *J. Power Sources*, 2007.
- [4] Y. C. Yang, P. H. Wang, Y. T. Tsai, and H. C. Ong, “Influences of feedstock and plasma spraying parameters on the fabrication of tubular solid oxide fuel cell anodes,” *Ceram. Int.*, 2018.
- [5] L. S. Wang, C. X. Li, C. J. Li, and G. J. Yang, “Performance of La_{0.8}Sr_{0.2}Ga_{0.8}Mg_{0.2}O₃-based SOFCs with atmospheric plasma sprayed La-doped CeO₂ buffer layer,” *Electrochim. Acta*, 2018.
- [6] D. Panuh, A. Muchtar, N. Muhamad, E. H. Majlan, and W. R. W. Daud, “Fabrication of thin Ag-YSB composite cathode film for intermediate- temperature solid oxide fuel cells,” *Compos. Part B Eng.*, 2014.
- [7] T. Talebi, M. Haji, and B. Raissi, “Effect of sintering temperature on the microstructure, roughness and electrochemical impedance of electrophoretically deposited YSZ electrolyte for SOFCs,” in *International Journal of Hydrogen Energy*, 2010.
- [8] M. S. Djošić, V. B. Miskovic-Stankovic, and V. V. Srdić, “Electrophoretic deposition and thermal treatment of boehmite coatings on titanium,” *J. Serbian Chem. Soc.*, vol. 72, no. 3, pp. 275–287, 2007.
- [9] A. Bodén, J. Di, C. Lagergren, G. Lindbergh, and C. Y. Wang, “Conductivity of SDC and (Li/Na)₂CO₃ composite electrolytes in reducing and oxidizing atmospheres,” *J. Power Sources*, vol. 172, no. 2, pp. 520–529, 2007.
- [10] T. Takahashi, T. Esaka, and H. Iwahara, “Conduction in Bi₂O₃-based oxide ion conductor under low oxygen pressure. II. Determination of the partial electronic conductivity,” *J. Appl. Electrochem.*, vol. 7, no. 4, pp. 303–308, 1977.
- [11] N. Jiang, E. D. Wachsman, and S. H. Jung, “A higher conductivity Bi₂O₃-based electrolyte,” *Solid State Ionics*, vol. 150, no. 3–4, pp. 347–353, 2002.
- [12] J. S. Ahn *et al.*, “High-performance bilayered electrolyte intermediate temperature solid oxide fuel cells,” *Electrochem. Commun.*, vol. 11, no. 7, pp. 1504–1507, 2009.
- [13] L. Zhang, L. Li, F. Zhao, F. Chen, and C. Xia, “Sm_{0.2}Ce_{0.8}O_{1.9}/Y_{0.25}Bi_{0.75}O_{1.5} bilayered electrolytes for low-temperature SOFCs with Ag-Y_{0.25}Bi_{0.75}O_{1.5} composite cathodes,” *Solid State Ionics*, vol. 192, no. 1, pp. 557–560, 2011.
- [14] A. V. Virkar, “Theoretical analysis of solid oxide fuel cells with two-layer, composite electrolytes: Electrolyte stability,” *J. Electrochem. Soc.*, vol. 138, no. 5, pp. 1481–1487, 1991.
- [15] S. Huang, G. Zhou, and Y. Xie, “Electrochemical performances of Ag-

- (Bi₂O₃)_{0.75}(Y₂O₃)_{0.25} composite cathodes,” *J. Alloys Compd.*, vol. 464, no. 1–2, pp. 322–326, 2008.
- [16] L. Zhang, C. Xia, F. Zhao, and F. Chen, “Thin film ceria-bismuth bilayer electrolytes for intermediate temperature solid oxide fuel cells with La_{0.85}Sr_{0.15}MnO_{3-δ}-Y_{0.25}Bi_{0.75}O_{1.5} cathodes,” *Mater. Res. Bull.*, vol. 45, no. 5, pp. 603–608, 2010.
- [17] T. Kenjo and Y. Kanehira, “Influence of the local variation of the polarization resistance on SOFC cathodes,” *Solid State Ionics*, vol. 148, no. 1–2, pp. 1–14, 2002.
- [18] S. Zha, Y. Zhang, and M. Liu, “Functionally graded cathodes fabricated by sol-gel/slurry coating for honeycomb SOFCs,” *Solid State Ionics*, vol. 176, no. 1–2, pp. 25–31, 2005.
- [19] E. D. Wachsman, G. R. Ball, N. Jiang, and D. A. Stevenson, “Structural and defect studies in solid oxide electrolytes,” *Solid State Ionics*, vol. 52, no. 1–3, pp. 213–218, 1992.
- [20] J. Y. Park and E. D. Wachsman, “Stable and high conductivity ceria/bismuth oxide bilayer electrolytes for lower temperature solid oxide fuel cells,” *Ionics (Kiel)*, vol. 12, no. 1, pp. 15–20, 2006.
- [21] Y. J. Leng and S. H. Chan, “Anode-supported SOFCs with Y₂O₃-doped Bi₂O₃/Gd₂O₃-Doped CEO₂ composite electrolyte film,” *Electrochem. Solid-State Lett.*, vol. 9, no. 2, pp. 10–14, 2006.

Graphite Coating of Aluminum Bipolar Plate Using Compression Molding Method

Rieza Zulrian Aldio¹, Dedikarni^{1, a)} and Deni Restu Fauzi¹⁾

¹*Department of Mechanical Engineering, Universitas Islam Riau, Pekanbaru, Indonesia*

a)corresponding author: dedikarni@eng.uir.ac.id

Abstract. Bipolar plate is one of the most important and quite expensive parts of Proton Exchange Membrane Fuel Cell (PEMFC). This research was conducted to compare the value of electrical conductivity, microstructure and flexural strength of the bipolar plate that acts as conductor based on the composition of the bipolar plate. The mass composition of the graphite and epoxy resin are at 60:40, 70-30 and 80-20 was used in compression molding process at 6 tons in 30 minutes. Electrical conductivity tests, microstructural observations and bending tests were carried out. It was found that the high electrical conductivity value at 50 S.cm⁻¹ and best microstructure surface in 80:20 specimen. As for the bending test, the highest value at 101.9MPa is found on 60:40 specimen. The results show that higher composition of graphite will elevate the electrical conductivity and higher composition of epoxy resin will elevate the bending test value of the aluminum bipolar plate.

INTRODUCTION

In a PEMFC system, bipolar plate has a critical role as the medium for water and hydrogen. These two are the source of the energy in fuel cell. PEMFC operates at low temperature and due to this, it requires pure hydrogen as the energy source [1]. With its low operating temperature and zero emissions, PEMFC became one of the most effective and popular source of energy [2-4]. Due to the low operating temperature, PEMFC also commonly refer to as low-temperature PEMFC (LT-PEMFC). Hence why the bipolar plate must have a good ability for conducting the electric.

Metals, due to its good electrical conductivity suited as the material for the bipolar plate. Metallic plate will produce better conductivity but at the same time it poses problems such as corrosion. Metallic material such as aluminum produce impressive electrical and thermal conductivity with also good mechanical properties [5]. From the economical point of view, it is not desirable to use metals for mass production. Even though the use of noble metal is a possibility, but again it is not feasible due to the cost. As an alternative, metallic polymer plate is developed to handle the corrosion problem while at the same time maintaining a good electrical conductivity.

Graphite is a well known material in the bipolar plate advancement. It exhibits good electrical and thermal conductivity [6], suitable to handle the corrosion problem at the cost of still lower conductivity compared to metals. Developing composite plate by adding graphite with metals were done in recent research and obtained better electrical conductivity and peak power output [7]. Several research utilizing Ti as a coating and found better corrosion resistance and electrical conductivity [8-9]. Graphite coating is utilized by methods such as injection molding, compression molding and etc depends on the materials used.

Compression molding is more fitting as manufacturing method of bipolar plate compared to machining process because the production cost is more expensive for machining. Machining process is gradually eliminated due to this reason [10], even though it is possible to applied machining process for the fabrication of the flow channel of a bipolar plate. For graphite coating aluminum process it is easier for the fabrication using compression method. This method is also popularly used for researching the effect of the varied composition of materials used for bipolar plate. The composition of the graphite into the aluminum will be researched. The composition ration will be between the graphite and epoxy resin that acts as the binder or adhesive.

METHOD

Materials and Equipments

These were the equipments used for supporting this research :

- a) Aluminum plate AA1100
- b) Specimen molding with the dimension of 12cmx12cmx1cm
- c) Amorphous Graphite produced by Evergreen Industries as the coating of the plate
- d) Epoxy resin as an adhesive

- e) Aquades water to remove dirt from the specimen
- f) Conductivity tester
- g) Olympus BX53M Microscope
- h) Bending machine

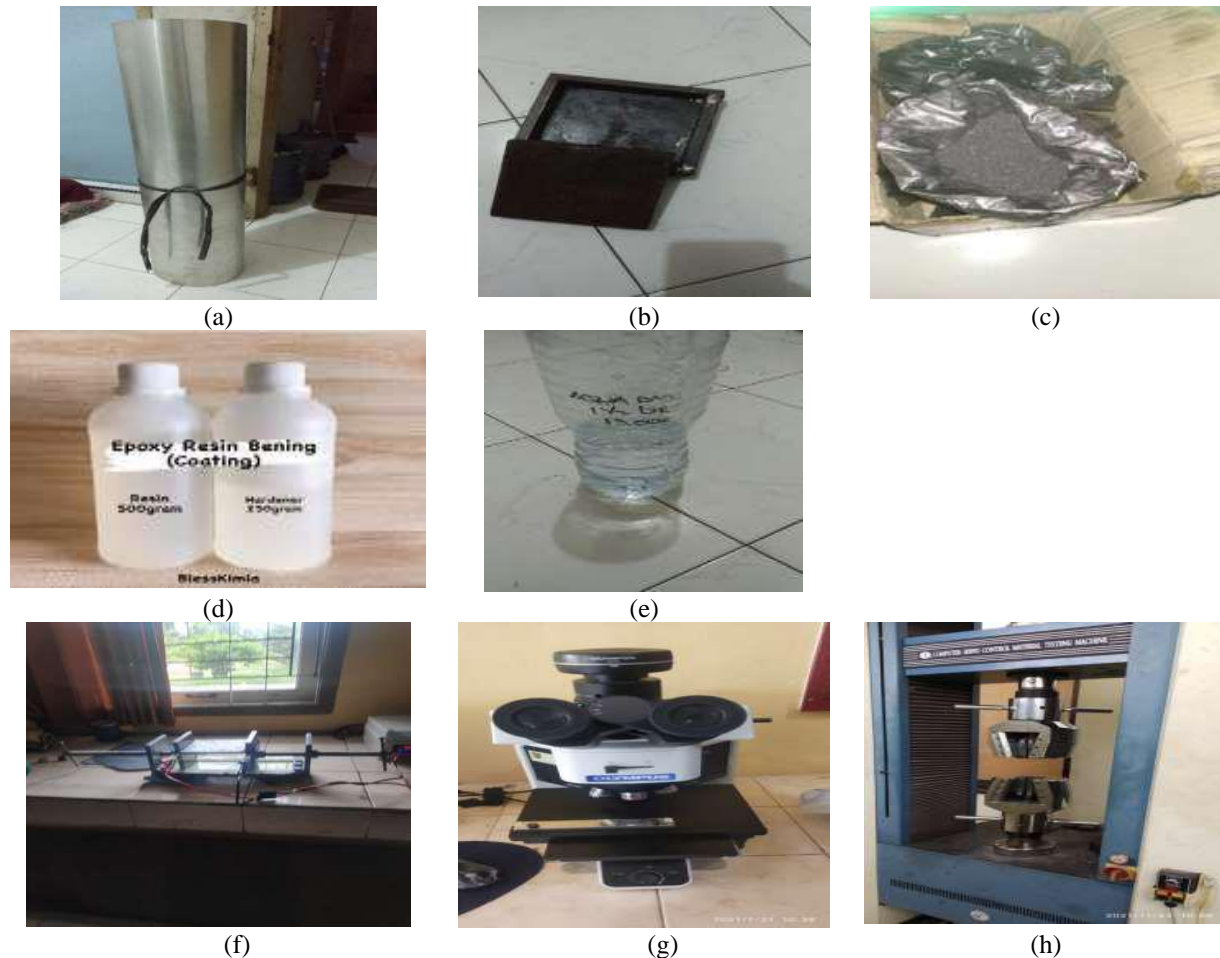


Figure 1. Materials and equipments in the research

Procedure

This research used aluminum plate that coated by graphite and epoxy resin as the specimen. Aluminum plate was put in the molding then coated and subjected to compression for coating process in a mold with dimension of 12cmx12cmx1cm. The compression molding were done with 6 ton force during 30 minutes. There were 3 types of composition between graphite and epoxy resin, namely were 60:40, 70:30 and 80:20 ratio based on the mass. The mass was calculated based on the volume of the mold and density of both graphite and epoxy resin.

When the specimens were collected from the mold, the specimens cleaned by aquade to remove any possible dirt. Some tests were carried out to determine the effect of the variation on the composition. The tests were electrical conductivity measured by conductivity tester using ASTM B193 standard, microstructure observation using Olympus microscope and bending test by bending machine. The tests are done in Laboratory of Department of Mechanical Engineering Universitas Islam Riau. All materials and equipment for the research are shown by figure 1a to 1h.

RESULTS AND DISCUSSIONS

Here are the results of the test on the specimens. There were 3 tests done, they were electrical conductivity, microstructure and bending test.

Electrical Conductivity Test

Table 1. Electrical conductivity of specimens

No	Composition (%)	Conductance (S)	Electrical Conductivity (S.cm-1)
1	60 : 40	142	14.2
2	70 : 30	250	25
3	80 : 20	500	50

Table 1 shows the average value of electrical conductivity of the 3 types of bipolar plate measured by the conductivity tester. The lowest value of electrical conductivity is at composition of 60:40 with 14.2Scm^{-1} and the highest is at composition 80:20 with value of 50Scm^{-1} . It is clear that the higher composition of graphite will increase the electrical conductivity of a plate. This could be resulted due to the nature of graphite that had good conductivity. Figure 3 below shows the trend of the electrical conductivity on different composition. There is a quite significant increase in conductivity between composition 70:30 to 80:20 compared with 60:40 to 70:30.

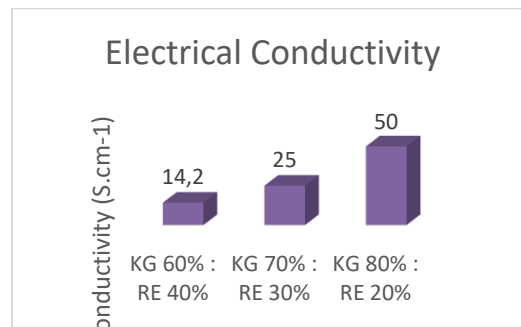


Figure 2. Electrical conductivity

Microstructure Observation

Microstructure observation on the 3 types of specimens are done. From figure 3, it is shown that there is uneven distribution of graphite of the specimen 60:40. This is due to the dominant use epoxy resin up to 40 percent and cause the spread of the graphite became not well distributed. This microstructure of specimen with 60:40 composition shows that the surface looks rough dan porous. All of these are cause by the amount of epoxy resin use in the specimen is dominant even though it only used at 40 percent of total.

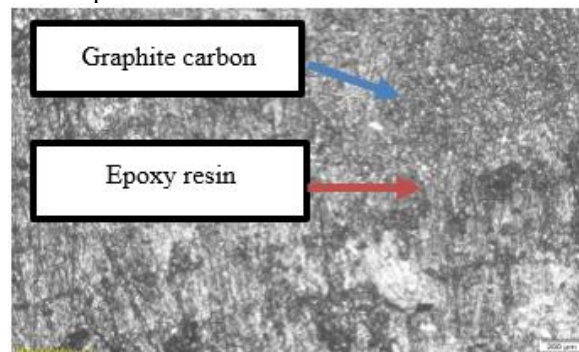


Figure 3. Microstructure of 60% graphite and 40% epoxy resin

The microstructure of 70:30 specimen is shown by figure 4. From the observation, it could be known that the particles of the graphite and epoxy resin are well and evenly distributed. This occur due to the larger amount of graphite used making the surface appears to be smoother. The result of 70:30 microstructure is different compared to the 60:40 with former being less porous than the latter.

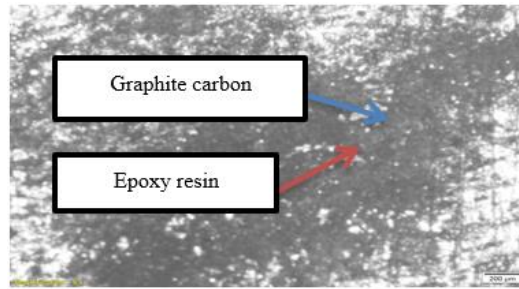


Figure 4. Microstructure of 70% graphite and 30% epoxy resin

The observation of the microstructure of specimen 80:20 is shown by figure 5. Higher composition of the graphite at 80% and lower epoxy resin at 20% cause better surface and particle's distribution. This specimen has the best distribution of particles and smoothest surface among all the specimens. While the epoxy resin did bind the aluminum and graphite, it is the increasing concentration of graphite that affect the distribution of particles and also the surface quality.

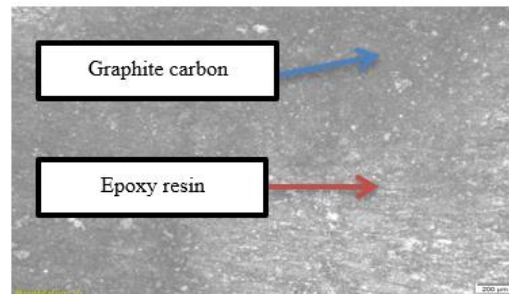


Figure 5. Microstructure of 80% graphite and 20% epoxy resin

Bending Test

The results of the bending test are done and table 2 below shows the value from each specimen.
Table 2. Bending test result

<u>Composition (%)</u>	<u>Area (Mm²)</u>	<u>Max. Force (MPa)</u>
60 : 40	464.400	101.9
70 : 30	635.100	65.3
80 : 20	623.200	21.9

Based on the table 2 above, the lowest value of the bending test is on the specimen with composition of 80:20 with 21.9 MPa and the highest is on specimen with composition of 60:40 with 101.9MPa. Specimen 70:30 has value in between the two of 60:40 and 80:20 with 65.3MPa. Figure 6 shows the trend of the increasing value of the bending test from specimens. It is seen that the increase use of the epoxy resin will also increase the bending test value of the specimen. Significant difference of bending test value between each specimen is noted in this graph. This occurred because the epoxy resin acts as the adhesive between aluminum and graphite. Hence, the increase of the epoxy resin will increase the bending value of an aluminum plate.

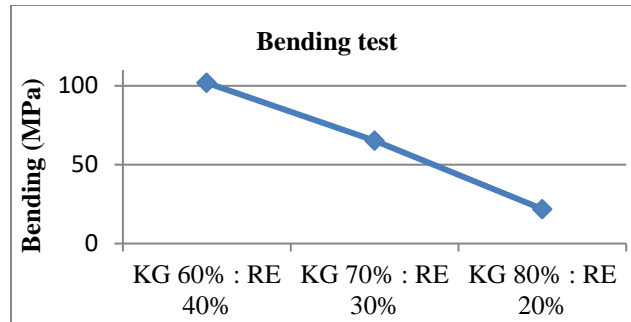


Figure 6. Bending test

CONCLUSION

In conclusion, the composition of the graphite and epoxy resin affects the electrical conductivity, microstructure and bending test of the aluminum plate. From the research, higher composition of graphite will increase the electrical conductivity, better particles distribution and surface quality. As for the epoxy resin, higher composition of it will increase the bending test value of the aluminum plate. For the future research, it is critical to find the right composition of graphite to obtain good electrical conductivity while at the same time getting good bending test value for the aluminum plate that used for fuel cell bipolar plate.

ACKNOWLEDGEMENT

The author would like to thank colleagues from the Department of Mechanical Engineering Universitas Islam Riau for supporting this research

REFERENCES

1. Igbala, M. Z., Rosli, M.I. and Panuh, D. *Performance Investigation of High-Temperature Proton Exchange Membrane Fuel Cell* (JURNAL KEJURUTERAAN, 2018), pp. 1-6.
2. Chen, Y., Enearu, O. L., Montalvao, D. & Sutharssan, T. *A Review of Computational Fluid Dynamics Simulations on PEFC Performance* (Journal of Applied Mechanical Engineering 5(6) 2016).
3. Heidary, H., Kermani, M.J. and Dabir, B. *Influences of bipolar plate channel blockages on PEM fuel cell performances* (Energy Convers. Manag. 124, 2016), pp. 51–60.
4. Zhiani, M., Kamali, S. and Majidi, S. *In-Plane Gas Permeability and Thought-Plane Resistivity of the Gas Diffusion Layer Influenced by Homogenization Technique and Its Effect on the Proton Exchange Membrane Fuel Cell Cathode Performance* (Int. J. Hydrogen Energy 41, 2016).
5. Madadi, F., Rezaeian, A., Edris, H. and Zhiani, M. *Improving Performance in PEMFC by Applying Different Coatings to Metallic Bipolar Plates* (Materials Chemistry and Physics 238 2019).
6. Hu, R., Tang, J., Zhu, G., Deng, Q. and Lu, J. *The Effect of Duty Cycle and Bias Voltage for Graphite-Like Carbon Film Coated 304 Stainless Steel as Metallic Bipolar Plate* (J Alloys Compd, 2019), pp.1067-78.
7. Lee M.H., Kim, H.Y., Oh, S.M., Kim, B.C., Bang, D. and Han, J.T. *Structural Optimization of Graphite for High-Performance Fluorinated Ethyleneepropylene Composites as Bipolar Plates* (Int J Hydrogen Energy, 2018).
8. Gao, P., Xie, Z., Wu, X., Ouyang, C., Lei, T. and Yang, P. *Development of Ti Bipolar Plates with Carbon/PTFE/Tin Composites Coating for PEMFCs* (Int J Hydrogen Energy, 2018).
9. Wang, J., Min, L., Fang, F., Zhang, W. and Wang, Y. *Electrodeposition of Graphene Nano-Thick Coating for Highly Enhanced Performance of Titanium Bipolar Plates in Fuel Cells* (Int J Hydrogen Energy, 2019, pp.16909-17).
10. Asri, N.F., Husaini, T., Sulong, A.B., Majlan, E.H. and Wan, R.W.D. *Coating of Stainless Steel and Titanium Bipolar Plates for Anticorrosion in PEMFC: a Review* (Int J Hydrogen Energy, 2017), pp.9135-48.